On the Differential Flatness and Control of Electrostatically Actuated MEMS

Guchuan Zhu, Jean Lévine, and Laurent Praly

Abstract— **Extending the stable travelling range of actuators forms one of the central topics in the control of electro-statically actuated MEMS. Though certain control schemes, such as charge control, capacitive feedback, and input-output linearization, can extend the travelling range to the full gap, the transient behavior of actuators is dominated by their mechanical dynamics. Thus, the performance may be poor if the natural damping of the devices is too low or too high. This paper presents an alternative for the control of parallel-plate electrostatic actuators, which combines the techniques of trajectory planning and robust nonlinear control. It is therefore capable of stabilizing the system at any point in the gap while ensuring desired performances. The simulation results demonstrate the advantage of the proposed control scheme.**

I. INTRODUCTION

This paper addresses the problem of control of a parallel-plate electrostatic actuator, which is one of the most commonly used devices in the application of micro-electromechanical systems (MEMS), such as mirrors, optical gratings, variable capacitors, and accelerometers [14].

It is well known that by applying a constant voltage across the plates, the stable travelling range of the moveable plate in this kind of devices is limited to one third of its full gap, the distance between the top plate and the bottom electrode when the voltage across the device equals zero [16]. Beyond that point, the moveable plate will suddenly and catastrophically snap to the fixed electrode, instantly reducing the gap to zero. This phenomenon is known as "pull-in" or "snap-down". Extending the travelling range of the moveable plate forms one of the central topics in the control of parallel-plate electrostatic actuators. This objective can be attained by modifying the mechanical configurations, such as leverage and nonlinear stiffening springs [7], [12]. Another approach is to use electrical sources other than simple voltage sources in order to nullify the effect of the increasing capacitance as the gap decreases, and then stabilizing the actuator beyond the pull-in limit. The techniques belonging to this category include using current drive source [13], [14], known also as charge control, and adding a series capacitance, representing a charge feedback, to the voltage control scheme [15]. Both

ways are capable of extending the travelling range to the full gap. An equilibrium beyond the pull-in position can eventually be stabilized by a closed-loop feedback control [3]. Recent researches have shown that the charge control and capacitor feedback, mentioned above, are effectively special cases of input-output linearization feedback control [10], [11].

Besides stabilizing the actuator around the set-point of operations, many applications of MEMS impose stringent requirements on the transient behavior of actuator, such as settling times, overshoots and oscillations. Furthermore, the control schemes should also be robust vis-à-vis manufactory tolerance, operation points, modeling errors, parameter uncertainties, and disturbances. It is indeed a very complex task to incorporate all the above factors into the design of control algorithms under the framework of linear control theory, and compromising the optimality of the system is inevitable [2].

The goal of this paper is to present a method for the design of control systems for electrostatically actuated MEMS, which can meet different performance requirements regardless of specific configurations. The considered problem is set-point control from any point in the gap to any other points between the electrodes. In the design of the controller, we use the method presented in [9], which combines the techniques of trajectory planning and robust nonlinear control. More precisely, based on differential flatness [5], [6], a feasible reference trajectory is constructed first in the phase plane, ensuring fast rise time while having well damped transient response. Then a robust closed-loop feedback control obtained by the potential method [1], [4] is added to the control scheme, that makes the reference trajectory an attractive invariant manifold.

The rest of the paper is organized as follows. Section II presents the model of a one degree of freedom (1DOF), parallel-plate electrostatic actuator. Section III demonstrates that such a system is differentially flat and, based on this property, an open-loop control under the framework of trajectory planning is constructed. In Section IV, a closed-loop control is proposed, while a reduced order observer, required for implementing the proposed control scheme due to the lack of speed measurement, is presented in Section V. Finally, the simulation results are reported in Section VI and Section VII contains some conclusions.

G. Zhu is with the Department of Electrical Engineering, École Polytechnique de Montréal, C.P. 6079, Succursale centre-ville, Montréal, QC, Canada H3C 3A7. (e-mail: `guchuan.zhu@polymtl.ca`).

J. Lévine and L. Praly are with Centre Automatique et Systèmes, École des Mines de Paris, 35 rue Saint Honoré, 77305 Fontainebleau cedex, France. (e-mail: `{jean.levine,laurent.praly}@ensmp.fr`).

II. MODELING OF ELECTROSTATIC ACTUATOR

The considered MEMS device is a one degree of freedom (1DOF), parallel-plate electrostatic actuator shown in Fig. 1.
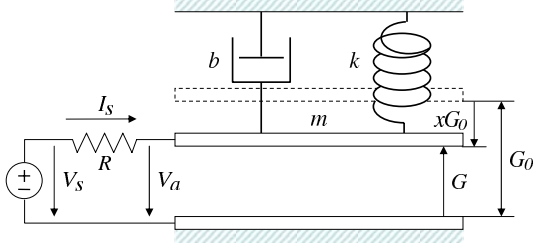
Fig. 1.   1DOF parallel-plate electrostatic actuator.

The mechanical part of the actuator can be represented as a spring-mass-dashpot assembly. The moveable upper electrode with a weight of m is attached to the fixed plate, being pulled by a spring with the elastic constant k, in a medium represented by a linear viscous damping coefficient b. The actuator is driven by a voltage source, and the corresponding scheme is called voltage control. Let $Q(t)$ be the charge on the device, $I_s(t)$ be the source current, $V_s(t)$ be the applied voltage, $V_a(t)$ be the actuation voltage, $G(t)$ be the air gap, G_0 be the zero voltage gap, A be the plate area, and ε be the permittivity in the gap. Then the capacitance of the device is:

$$C(t) = \frac{\varepsilon A}{G(t)}, \tag{1}$$

and the attractive electrostatic force on the moving plate is:

$$F(t) = \frac{Q^2(t)}{2\varepsilon A} = \frac{\varepsilon A V_a^2}{2G^2(t)}. \tag{2}$$

Thus the equation of motion is given by:

$$m\ddot{G}(t) + b\dot{G}(t) + k(G(t) - G_0) = -\frac{Q^2(t)}{2\varepsilon A}. \tag{3}$$

Assuming the system started operating from an initially uncharged state at $t = 0$, then the charge in the electrodes at the time t is:

$$Q(t) = \int_0^t I_s(\tau)d\tau, \tag{4}$$

or equivalently

$$\dot{Q}(t) = I_s(t). \tag{5}$$

The current through the resistor R can be obtained by a simple application of Kirchhoff's Voltage Law and reads [16]:

$$\dot{Q}(t) = \frac{1}{R}\left(V_s(t) - \frac{Q(t)G(t)}{\varepsilon A}\right). \tag{6}$$

In general, the input current $I_s(t)$ and the voltage across the device, $V_a(t) = Q(t)G(t)/\varepsilon A$, are available for measurement. Since they differ only by the input voltage, it is sufficient to consider either of them. Accurate measurement of capacitance across the device, $C(t)$, is also possible. Therefore the charge on the device, $Q(t)$, can be deduced from the above. From the measurement of voltage and capacitance, it is also possible to compute the gap between the electrodes, $G(t)$. Note that it is possible to measure the

charge directly without using the capacitance by inserting in series a fixed capacitor. This is how charge feedback is implemented in the case of capacitive stabilization.
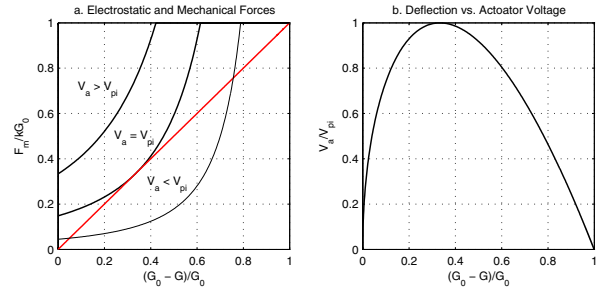

Fig. 2.   Saddle node bifurcation w.r.t. equilibrium voltage V_a^*.

From (2) and (3) it can be seen that the electrostatic force F increases with the inverse square of gap, while restoring mechanical force (the third term in the left hand side of (3)) increases linearly with the plate deflection. As shown in Fig. 2, there is a critical value for the voltage across the device, $V_{pi} = \sqrt{8kG_0^2/27C_0}$, for that if the equilibrium voltage $V_a^* < V_{pi}$, there are two equilibrium points in the gap, lying in $[0, \frac{2}{3}G_0]$ and $[\frac{2}{3}G_0, G_0)$ respectively. Whereas if $V_a^* = V_{pi}$, there is only one equilibrium point at the one third of the gap. And finally, if $V_a^* > V_{pi}$, then there is no equilibrium, and the system is dominated by the electrostatic force. The equilibrium at one third of the gap is the so-called *pull-in* or *snap-down* position and the corresponding equilibrium voltage, V_{pi}, the *pull-in* or *snap-down* voltage. It can be shown that all equilibria beyond the pull-in position are unstable. Therefore, in terms of bifurcation theory, this critical point corresponds to a saddle-node bifurcation with respect to equilibrium voltage. Consequently, with a constant voltage control, the travelling range of the actuator is limited to one third of its full gap.

To make the system analysis and control design easier, we transform the system (3)-(6) into normalized coordinates by changing the time scale, $\tau = \omega_0 t$, and performing a normalization as follows [13]:

$$x = 1 - \frac{G}{G_0}, \; q = \frac{Q}{Q_{pi}}, \; u = \frac{V_s}{V_{pi}}, \; i = \frac{I_s}{V_{pi}\omega_0 C_0}, \; r = \omega_0 C_0 R, \tag{7}$$

where $C_0 = \varepsilon A/G_0$ is the capacitance at rest, $Q_{pi} = \frac{3}{2}C_0 V_{pi}$ the pull-in charge corresponding to the pull-in voltage, $\omega_0 = \sqrt{\frac{k}{m}}$ the undamped natural frequency, and $\zeta = \frac{b}{2m\omega_0}$ the damping ratio.

Accordingly, the normalized voltage across the actuator can be expressed in terms of the normalized deflection of the moveable electrode:

$$u_a = \frac{3}{2}q(1-x), \tag{8}$$

and the dynamics of normalized charge becomes:

$$\dot{q} = \frac{2}{3}i. \tag{9}$$

2494

Let $v = \dot{x}$ be the speed of deflection of the moveable electrode, then the system (3) and (6) can be written in the normalized coordinates as:

$$
\begin{cases}
\dot{x} = v \\
\dot{v} = -2\zeta v - x + \dfrac{1}{3}q^2 \\
\dot{q} = \dfrac{2}{3r}\left(u - \dfrac{3}{2}q(1-x)\right)
\end{cases}, \qquad (10)
$$

which is defined on the state space $\chi = \{(x,v,q) \subset \mathbb{R}^3 \mid x \in [0,1],\ q \geq 0\}$. Note that the normalized deflection always ranges from 0 to 1. In the case where the thickness of the insulating material coated on the bottom plate should be taken into account [10], [11], it suffices to incorporate this factor with the variable transformation while normalizing the deflection.

It can be seen that in the new coordinates, the mechanical subsystem has a damping ratio ζ and a undamped natural frequency of 1.

Since in what follows we will deal only with normalized quantities, we can use t to denote the time and omit the qualifier "normalized" while not causing any confusion.

III. FLATNESS AND TRAJECTORY PLANNING

Like many mechatronic systems, electrostatically actuated MEMS are differentially flat. More precisely, the system (10) is flat with x as flat output. Therefore all of the remaining states, as well as the input in (10) can be obtained from x and its derivatives until an appropriate order is reached [5], [6]. Thus it is possible to compute any trajectory of the system without integrating the corresponding differential equations. In fact, expressing the trajectory with respect to time is nowhere needed. On the contrary, it is more convenient to express the desired trajectory with respect to x, because that allows the trajectory generation to be time independent. Hence, the controller will work in an auto-scheduling fashion. We remark also that if the reference trajectory is such that y_r has a monotonic behavior then we can use x itself as a parameter instead of time. Moreover, by eliminating the time from (10), the new system is flat with respect to v (now a function of x). To see that, we rewrite (10) as:

$$
\begin{cases}
vv' = -2\zeta v - x + \dfrac{1}{3}q^2 \\
vq' = \dfrac{2}{3r}\left(u - \dfrac{3}{2}q(1-x)\right)
\end{cases} \qquad (11)
$$

where $v' = \dfrac{dv}{dx}$ and $q' = \dfrac{dq}{dx}$. Thus,

$$
q^2 = 3vv' + 6\zeta v + 3x \qquad (12)
$$

and

$$
u = \frac{3}{2}(rvq' + q(1-x)). \qquad (13)
$$

Since

$$
q' = \frac{3}{2q}(2\zeta v' + v'^2 + vv'' + 1) \qquad (14)
$$

is also a function of v, v' and v'', with $v'' = \frac{dv'}{dx} = \frac{d^2v}{dx^2}$, we have proved that q and u can be expressed as functions of x, v, v' and v'', and thus that the system (11) is flat. Furthermore, in the new coordinates, the current can be expressed as

$$
i = \frac{3}{2}vq', \qquad (15)
$$

which is obviously a function of v, v' and v''.

Note that because the flatness of electrostatic actuators is independent of the control schemes, this property holds for both charge and voltage controlled devices.

The system (11) being flat, any of its trajectory may be expressed as a function of the corresponding trajectory $x \mapsto v(x)$ of the flat output.

It is now convenient to denote by θ, ρ and μ the functions $x \mapsto v$, $x \mapsto q$, and $x \mapsto u$ respectively, to avoid confusion with the time functions. The trajectory planning problem now consists in determining the curve $x \mapsto \theta(x)$.

The desired trajectory $x \mapsto \theta(x)$ may therefore be obtained, by interpolation, as a 5th degree polynomial:

$$
\theta(x) = a_0 + a_1\xi(x) + a_2\xi^2(x) + a_3\xi^3(x) + a_4\xi^4(x) + a_5\xi^5(x), \qquad (16)
$$

where $\xi(x) = \frac{x - x_i}{X}$ with $X = x_f - x_i$. The coefficients in (16) can be obtained by applying the initial and final conditions and the results are:

$$
a_0 = 0, \quad a_1 = Xv'(x_i), \quad a_2 = \frac{1}{2}X^2v''(x_i).
$$

$$
a_3 = -6Xv'(x_i) - \frac{3}{2}X^2v''(x_i) - 4Xv'(x_f) + \frac{1}{2}X^2v''(x_f),
$$

$$
a_4 = 8Xv'(x_i) + \frac{3}{2}X^2v''(x_i) + 7Xv'(x_f) - X^2v''(x_f), \quad (17)
$$

$$
a_5 = -3Xv'(x_i) - \frac{1}{2}X^2v''(x_i) - 3Xv'(x_f) + \frac{1}{2}X^2v''(x_f).
$$

Since

$$
\dot{v} = vv',
$$
$$
\ddot{v} = 2vv'^2 + v^2v'',
$$

the initial and final constraints on the trajectory will be respected as long as

$$
|v'(x_i)| < \infty, \quad |v'(x_f)| < \infty, \quad |v''(x_i)| < \infty, \quad |v''(x_f)| < \infty.
$$

The free parameters $v'(x_i)$, $v''(x_i)$, $v'(x_f)$, and $v''(x_f)$ can be chosen, for example, to make the reference trajectory to fit performance specifications, under constraints on drive current and applied voltage.

Notice that since all the time derivatives of x have to vanish at the equilibria, the desired trajectory can be represented by a polynomial with an arbitrary, finite order. The resulting system is equivalent to the original one in the sense of Lie-Bäcklund [6], while allowing the addition of more degrees of freedom in trajectory tuning and the obtaining of the desired behavior (e.g. fast rise time, low overshoot, and well damped oscillations). Note also that the pull-in equilibrium point is removed in this approach since we are using time-varying controls that exactly generate

2495

the required polynomial reference trajectory of $v(x)$. This remark will even be enhanced in the next section by a closed-loop synthesis that makes the reference trajectory tracking stable.

IV. CONTROL SYNTHESIS

A closed-loop control is required in our scheme in order to stabilize the system along any reference trajectory. In addition, the closed-loop control will make the system robust vis-à-vis modeling errors, parameter uncertainties, and disturbances. Obviously, the function (θ, ρ) previously designed defines an invariant set of system (10). Indeed, for any initial condition (x, v, q) satisfying:

$$(v, q) = (\theta(x), \rho(x)), \tag{18}$$

the input:

$$u = \mu(x) \tag{19}$$

satisfies (10) and is such that the corresponding solution $(x(t), v(t), q(t))$ satisfies for all t:

$$(v(t), q(t)) = (\theta(x(t)), \rho(x(t))). \tag{20}$$

Moreover, this trajectory coincides with the planned reference trajectory.

On this set, the dynamics of system (10) reduce to:

$$\dot{x} = \theta(x). \tag{21}$$

Outside this set, we have:

$$\dot{x} = v = \theta(x) + (v - \theta(x)) = \theta(x) + e_v. \tag{22}$$

Thus, in order that the trajectory of the dynamic system (10) converge to the planned reference trajectory, it suffices to asymptotically stabilize the invariant set $v = \theta(x)$. According to (11),

$$
\begin{aligned}
\dot{e}_v &= \left(-2\zeta v - x + \frac{1}{3}q^2 \right) - \theta'(x)v \\
&= \theta(x)\theta'(x) - \frac{1}{3}\rho^2(x) + 2\zeta\theta(x) + x \\
&\quad - 2\zeta v - x + \frac{1}{3}q^2 - \theta'(x)v \\
&= -(2\zeta + \theta'(x))e_v - \frac{1}{3}(\rho(x) + q)(\rho(x) - q). \tag{23}
\end{aligned}
$$

By adding and removing a term $\frac{1}{3}g(x)e_v(\rho(x) + q)$ to and from (23), we obtain

$$
\begin{aligned}
\dot{e}_v = & -(2\zeta + \theta'(x) + \frac{1}{3}g(x)(\rho(x) + q))e_v \\
& - \frac{1}{3}(\rho(x) + q)(\rho(x) - q - g(x)e_v). \tag{24}
\end{aligned}
$$

In order to stabilize (24), we impose

$$\dot{e}_q = -k_0 e_q + \frac{1}{3}(\rho(x) + q)e_v \tag{25}$$

where

$$e_q = \rho(x) - q - g(x)(v - \theta(x)).$$

Consider now the following Lyapunov function candidate:

$$V(x, v, q) = \frac{1}{2}e_v^2 + \frac{1}{2}e_q^2.$$

The time derivative of $V(x, v, q)$ along the solutions of system (24) and (25) is

$$
\begin{aligned}
\dot{V}(x, v, q) &= \dot{e}_v e_v + \dot{e}_q e_q \\
&= -\eta(x, q)e_v^2 - k_0 e_q^2.
\end{aligned}
$$

where

$$\eta(x, q) = 2\zeta + \theta'(x) + \frac{1}{3}g(x)(\rho(x) + q). \tag{26}$$

Since $\rho(x)$ is positive for all $x \in (0, 1]$ and q is non negative, by choosing $g(x)$ as a constant given by

$$g_0 \geq 3 \sup_{x \in (0, 1]} \left(\frac{|\theta'(x)|}{\rho(x)} \right), \tag{27}$$

$\eta(x, q)$ will be a positive function. It is clear that $\dot{V}(x, v, q)$ will be negative definite for any $k_0 > 0$. Hence the error dynamics (24) and (25) are asymptotically stable provided that g_0 is chosen as (27) and $k_0 > 0$, and the reference trajectory is an asymptotically attractive one.

Finally, the control signal can be deduced from (25), which is given as

$$
\begin{aligned}
u = & \, \mu(x) \\
& + \frac{3r}{2}\left(\left(k_0 + \frac{1}{3}g_0(\rho(x) + q) \right)e_q + \frac{1}{r}(1 - x)(q - \rho(x)) \right. \\
& \left. + \left(g_0 \left(2\zeta + \theta'(x) + \frac{1}{3}g_0(\rho(x) + q) \right) + \rho'(x) \right)e_v \right). \\
& \tag{28}
\end{aligned}
$$

V. SPEED OBSERVER DESIGN

Since directly sensing the velocity v during the normal operation of the device is extremely difficult, if not impossible, we need to construct a speed observer in order to provide the estimate of v required for implementing the closed-loop control described in the previous section. It can be shown that system (10) with the deflection and the charge as outputs admits the observer canonical form [8]. Therefore it is possible to find a full order observer with linear error dynamics. However, we need only to directly construct a reduced order speed observer. To this aim, we set:

$$z = v - k_v x \tag{29}$$

where k_v is an arbitrary positive real number. Differentiating (29), we get

$$\dot{z} = -((2\zeta + k_v)k_v + 1)x - (2\zeta + k_v)z + \frac{1}{3}q^2. \tag{30}$$

Thus, if we set

$$\hat{z} = \hat{v} - k_v x$$

where $\hat{v}$ is the required estimate of v and $\hat{z}$ the one of z, then

$$\dot{\hat{z}} = -((2\zeta + k_v)k_v + 1)x - (2\zeta + k_v)\hat{z} + \frac{1}{3}q^2. \tag{31}$$

2496

Let $e = \hat{z} - z = \hat{v} - v$ denote the estimation error, and note that $\frac{d}{dt}(\hat{z} - z) = \frac{d}{dt}(\hat{v} - v) = \dot{e}$. The error dynamics can be deduced from (30) and (31):

$$\dot{e} = -(2\zeta + k_v)e \qquad (32)$$

and is globally exponentially stable at the origin with a decay rate defined by k_v. This implies that

$$\hat{v} = \hat{z} + k_v x \qquad (33)$$

and (31) form an exponential observer.

VI. EXAMPLES AND SIMULATION RESULTS

Assuming for an electrostatic actuator that the dynamics of the electrical subsystem are much faster than the ones of the mechanical subsystem, then the behavior of the actuator will be dominated by the latter. This situation can be produced by using an ideal current source in a charge control scheme that can deliver the required amount of charge to the device in a sufficiently small time period before the top plate starts to move [13], [14]. The same result can also be obtained by using an input-output linearization control [10], in that the mechanical subsystem is nothing but the zero dynamics. Fig. 3 shows the responses corresponding to a deflection of 100% gap of three systems with damping ratio of 0.2, 1 and 5, respectively, driven by an ideal current source. Clearly, the system with high damping ratio suffers from a long settling time, while the one with low damping ratio suffers from oscillation and important overshoot. Note that when the set-point is close to the full gap position, the overshoot will drive the moveable plate to hit the fixed electrode. The unexpected contact between two plates could damage the surface of the electrodes and reduce the lifetime of the device. The response of the system with a damping ratio of 1 yields desired behavior: fast rise time and no overshoot or oscillation. This performance may however be too demanding for other systems. The nominal system used in trajectory planning is thus the one with a damping ratio of 1.5.
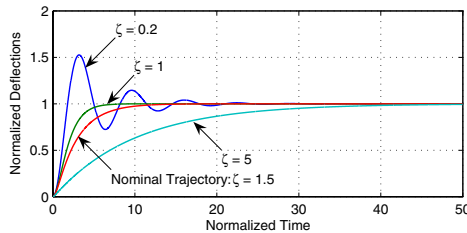

Fig. 3. Responses of parallel-plate electrostatic actuators driven by an ideal current source.

The function of displacement speed of the moveable plate versus the deflection of the nominal system is drawn in Fig. 4.a, from which $v'(x_i)$, $v''(x_i)$, $v'(x_f)$, and $v''(x_f)$ can be deduced, and the reference trajectory (16) can be determined. The obtained reference trajectories corresponding to different deflections are shown in Fig. 4.b.
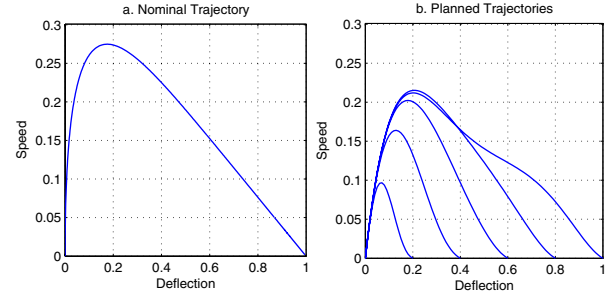

Fig. 4. Nominal and planned trajectories.

Fig. 5.a shows the responses of a parallel-plate electrostatic actuator controlled by the proposed scheme with damping ratio $\zeta = 1$, corresponding to the deflections of 20%, 40%, 60%, 80%, and 100% of full gap, respectively. The normalized resistance is chosen to be 1. A pulse voltage with a width of 0.2 and an amplitude of 2, both in normalized coordinates, is applied to steer the operation. The actuation voltages during the operation are also sketched. Note that the actuator is supposed to be controlled by a bi-polar voltage source, whose amplitude is limited to ± 3 (normalized unit) by a saturator.
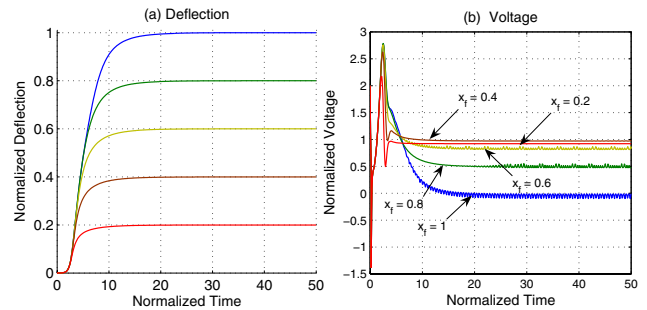

Fig. 5. Actuation voltages and responses of a voltage controlled parallel-plate electrostatic actuator with damping ratio $\zeta = 1$.

Fig. 6 shows the responses of voltage controlled parallel-plate electrostatic actuators with damping ratio $\zeta = 0.1$, $\zeta = 1$ and $\zeta = 5$, corresponding to a deflection of 20%, 40%, 60%, 80%, and 100% of full gap, respectively. Comparing with the ideal current drive scheme (see Fig. 3), the performance of the system is considerably improved.
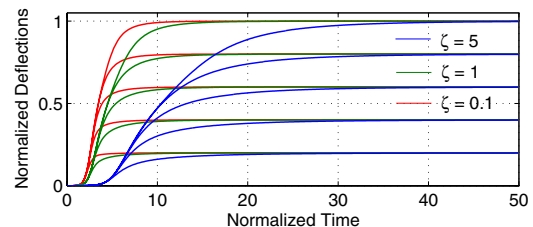

Fig. 6. Responses of voltage controlled parallel-plate electrostatic actuators with system parameter variations.

2497

The last test shows the capability of the designed electrostatic actuator to reject the disturbances caused by, for example, vibrations. A disturbance in the position with an amplitude of 5% of full gap is applied after the actuator has been stabilized at the equilibrium, 50% of full gap in this example. The damping ratio of the system is 0.1. The simulation result (see Fig. 7) shows that the system recovers well from the disturbance. A high actuation voltage is however observed. This is due to the high value of the controller gain. If the actuation voltage exceeds the level of actuator authority, this factor must be incorporated into the controller gain tuning.
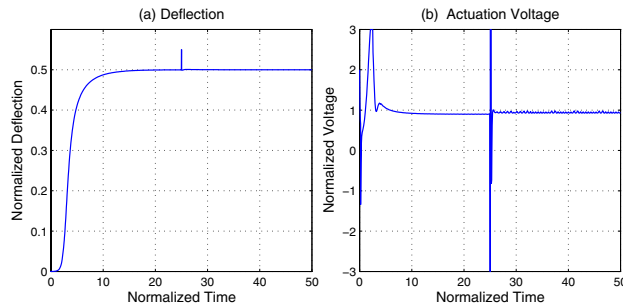

Fig. 7. Disturbance rejection.

Note that all the reported results are obtained by using the same controller, whose design is based on the nominal plant ($\zeta = 1.5$). This shows the robustness of the presented control scheme.

VII. CONCLUSIONS

This paper addressed the control of a parallel-plate electrostatic actuator. It has been shown that this system is differentially flat, and based on this property, a control scheme, combining trajectory planning and nonlinear robust control has been presented. The obtained control system exhibited an excellent performance in terms of response time, overshoot, and damping oscillations, and was robust vis-à-vis the dynamical characteristics of the device. Extending the presented method to more realistic devices, where the parasitic parameters are not negligible, and to multi-degree of freedom devices may be the subject of further research. Other specific applications of MEMS, such as scanning micro-mirrors, deserve more attention and will be addressed in the future.

VIII. ACKNOWLEDGMENTS

REFERENCES

[1] A.A. Andronov, A.A. Vitt, and S.E. Khaikin, *Theory of oscillators*, Dover, 1987.
[2] J. Bryzek and E.Abbott, "Control Issues for MEMS", *Proc. of the 42nd IEEE Conference on Decision and Control*, Maui, Hawaii, pp. 3039-3047, December 2003.
[3] P.B. Chu, and K.S.J. Pister, "Analysis of closed-loop control of parallel-plate electrostatic microgrippers", *Proc. IEEE Int. Conf. Robotics and Automation*, pp. 820-825, 1994.
[4] J.-M. Coron, L. Praly, and A. Teel. "Feedback stabilization of nonlinear systems: Sufficient conditions and Lyapunov and input-output techniques". Minicourse on Stabilization of nonlinear system, L. Praly (Organizer). *In Trends in Control*, A. Isidori (Editor), Springer Verlag, pp.293-347, August 1995.
[5] M. Fliess, J. Lévine, P. Martin, and P. Rouchon, "Flatness and defect of non-linear systems: Introductory theory and examples", *International Journal of Control*, Vol. 61, pp. 1327-1361, 1995.
[6] M. Fliess, J. Lévine, P. Martin, and P. Rouchon, "A Lie-Bäcklund approach to equivalence and flatness of nonlinear systems", *IEEE Trans. on Automatic Control*, vol. 44, No. 5, pp. 922-937, 1999.
[7] E. S. Hung and S. D. Senturia, "Extending the travel range of analog-tuned electrostatic actuators", *Journal of Microelectromechanical Systems*, vol. 8, pp. 497-505, Dec. 1999.
[8] A. Isidori, *Nonlinear Control Systems*, 3rd Edition. Springer-Verlage, London 1995.
[9] J. Lévine, L. Praly, and E. Sedda, "On the control of an electro-magnetic actuator of valve positionning on a camless engine", *Proc. AVEC 04*, Arnhem, The Netherlands, August 2004.
[10] D.H.S. Maithripala, J.M. Berg, and W.P. Dayawansa, "Capacitive Stabilization of an Electrostatic Actuator: An Output Feedback Viewpoint", *Proc. of the 2003 American Control Conference*, Denver, CO, pp. 4053-4058, June 4-6, 2003.
[11] D.H.S. Maithripala, J.M. Berg, and W.P. Dayawansa, "Nonlinear Dynamic Output Feedback Stabilization of Electostatically Actuated MEMS", *Proc. of the 42nd IEEE Conference on Decision and Control*, Maui, Hawaii, pp. 61-66, December 2003.
[12] Y. Nemirovsky and O. Bochobza-Degani, "A methodology and model for the pull-in parameters of electrostatic actuators", *Journal of Microelectromechanical Systems*, vol. 10, no. 4, pp. 601-615, Dec. 2001.
[13] J. Pont-Nin, A. Rodríguez, and L.M. Castañer, "Voltage and Pull-In Time in Current Drive of Electrostatic Actuators", *Journal of Microelectromechanical Systems*, Vol. 11, No. 3, pp. 196-205, 2002.
[14] J.I. Seeger and B.E. Boser, "Charge Control of Parallel-Plate, Electrostatic Actuators and the Tip-In Instability", *Journal of Microelectromechanical Systems*, Vol. 12, No. 5, pp. 656-671, 2003.
[15] J.I. Seeger and S.B. Crary, "Stabilization of electrostatically actuated mechanical devices", in *Tech. Dig. 9th Int. Conf. Solid-State Sensors and Actuators (Transducers' 97)*, pp. 1133-1136, June 1997.
[16] S.D. Senturia, *Microsystem Design*, Kluwer Academic Publishers, Norwell, MA 2001.